

Supporting information

Highly Efficient Non-Doped Blue Organic Light Emitting Diodes Based On D- π -A Chromophore with Different Donor Moieties

Venugopal Thanikachalam*, Palanivel Jeeva, Jayaraman Jayabharathi

Department of Chemistry, Annamalai University, Annamalainagar 608 002, Tamilnadu, India

* Address for correspondence

Dr. V. Thanikachalam
Professor of Chemistry
Department of Chemistry
Annamalai University
Annamalainagar 608 002
Tamilnadu, India.
Tel: +91 9488476098
E-mail: vtchalam2005@yahoo.com

Contents

SI-I: Solvatochromic Experiments

SI-II: Charge–Transfer Intexes

SI-III: Figures

SI-IV: Schemes

SI-V: Tables

SI-I: Solvatochromic Experiments

According to Lippert–Mataga equation the dipole moment can be estimated from the slope of the plot of Stokes shift ($\tilde{\nu}_{\text{abs}} - \tilde{\nu}_{\text{flu}}$) against solvent polarity function $f(\epsilon, n)$,

$$\text{hc}(\tilde{\nu}_{\text{abs}} - \tilde{\nu}_{\text{flu}}) = \text{hc}(\frac{\text{hc}\tilde{\nu}_{\text{abs}}^{\text{vac}}}{\tilde{\nu}_{\text{abs}}} - \frac{\text{hc}\tilde{\nu}_{\text{flu}}^{\text{vac}}}{\tilde{\nu}_{\text{flu}}}) + 2 (\mu_e - \mu_g)^2 / a_o^3 [(\epsilon - 1/2 \epsilon + 1) - \frac{1}{2} (n^2 - 1/2 n^2 + 1)], \text{ where}$$

μ_g and μ_e are ground and excited state dipole moments respectively, $\tilde{\nu}_{\text{abs}}$ and $\tilde{\nu}_{\text{abs}}^{\text{vac}}$ are the spectral positions of a solvent-equilibrated absorption maxima and extrapolated to gas-phase, $\tilde{\nu}_{\text{flu}}$ and $\tilde{\nu}_{\text{flu}}^{\text{vac}}$ are the spectral positions of the solvent equilibrated fluorescence maxima and extrapolated to the gas-phase, respectively, a_o is Onsager radius and ϵ and n are the dielectric constant and refractive index of the solvent, respectively.

The fitted results show that the non-linear correlation between Stokes shift and solvent polarity function. Estimation of free energy change of salvation (ΔG_{solv}) and reorganization energies (λ) in various solvents are displayed in Tables S6 and S7. Marcus shown that $E(A) = \Delta G_{\text{solv}} + \lambda_1$ and $E(F) = \Delta G_{\text{solv}} - \lambda_0$; $E(A) + E(F) = 2\Delta G_{\text{solv}}$; $E(A) - E(F) = 2\lambda$ (under, $\lambda_0 \approx \lambda_1 \approx \lambda$), where $E(A)$ and $E(F)$ are absorption maxima and fluorescence maxima in cm^{-1} , respectively, ΔG_{solv} is difference in free energy of ground and excited states in a given solvent and λ is reorganization energy. The difference between ΔG_{hex} and ΔG_{sol} gives the free energy change required for hydrogen bond formation. The plot of $\Delta (\Delta G_{\text{solv}})$ against $f(\epsilon, n)$ has been shown in Figure S6. The definite reorganization energies confirmed the interaction between low frequency motions such as reorientation of solvent cell with low and medium frequency nuclear motion of the solute.

SI-II: Charge–Transfer Intexes

The hole–particle pair interactions have been related to the distance covered during the excitations one possible descriptor Δr intex could be used to calculate the average distance which is weighted in function of the excitation coefficients.

$$\Delta r = \frac{\Sigma_{ia} k_{ia}^2 |\langle \varphi_a | r | \varphi_a \rangle - \langle \varphi_i | r | \varphi_i \rangle|}{\Sigma_{ia} K_{ia}^2} \quad \dots \quad (\text{S1})$$

where $|\langle \varphi_i | r | \varphi_i \rangle|$ is the norm of the orbital centroid [1–4]. Δr -index will be expressed in Å.

The density variation associated to the electronic transition is given by

$$\Delta\rho(r) = \rho_{EX}(r) - \rho_{GS}(r) \quad \dots \quad (\text{S2})$$

where $\rho_{GS}(r)$ and $\rho_{EX}(r)$ are the electronic densities of to the ground and excited states, respectively. Two functions, $\rho_+(r)$ and $\rho_-(r)$, corresponds to the points in space where an increment or a depletion of the density upon absorption is produced and they can be defined as follows:

$$\rho_+(r) = \begin{cases} \Delta\rho(r) & \text{if } \Delta\rho(r) > 0 \\ 0 & \text{if } \Delta\rho(r) < 0 \end{cases} \quad \dots \quad (\text{S3})$$

$$\rho_-(r) = \begin{cases} \Delta\rho(r) & \text{if } \Delta\rho(r) < 0 \\ 0 & \text{if } \Delta\rho(r) > 0 \end{cases} \quad \dots \quad (\text{S4})$$

The barycenters of the spatial regions R_+ and R_- are related with $\rho_+(r)$ and $\rho_-(r)$ and are shown as

$$R_+ = \frac{\int r \rho_+(r) dr}{\int \rho_+(r) dr} = (x_+, y_+, z_+) \quad \dots \quad (\text{S5})$$

$$R_- = \frac{\int r \rho_-(r) dr}{\int \rho_-(r) dr} = (x_-, y_-, z_-) \quad \dots \quad (\text{S6})$$

The spatial distance (D_{CT}) between the two barycenters R_+ and R_- of density distributions can thus be used to measure the CT excitation length

$$D_{CT} = |R_+ - R_-| \quad \dots \quad (\text{S7})$$

The transferred charge (q_{CT}) can be obtained by integrating over all space $\rho_+ (\rho_-)$,. Variation in dipole moment between the ground and the excited states (μ_{CT}) can be computed by the following relation:

$$\|\mu_{CT}\| = D_{CT} \int \rho_+(r) dr = D_{CT} \int \rho_-(r) dr \quad \dots \dots \dots \quad (S8)$$

$$= D_{CT} q_{CT} \dots \quad (S9)$$

The difference between the dipole moments $\|\mu_{CT}\|$ have been computed for the ground and the excited states $\Delta\mu_{ES-GS}$. The two centroids of charges (C^+/C^-) associated to the positive and negative density regions are calculated as follows. First the root-mean-square deviations along the three axis (σ_{aj} , $j = x, y, z$; $a = +$ or $-$) are computed as

$$\sigma_{a,j} = \sqrt{\frac{\sum_i \rho_a(r_i) (j_i - j_a)^2}{\sum_i \rho_a(r_i)}} \quad \dots \quad (\text{S10})$$

The two centroids (C_+ and C_-) are defined as

$$C_+(r) = A_+ e^{\left(-\frac{(x - x_+)^2}{2\sigma_{+x}^2} - \frac{(y - y_+)^2}{2\sigma_{+y}^2} - \frac{(z - z_+)^2}{2\sigma_{+z}^2} \right)} \quad \dots \quad (\text{S11})$$

$$C_{-+}(r) = A_- e \left(-\frac{(x - x_-)^2}{2\sigma_x^2} - \frac{(y - y_-)^2}{2\sigma_y^2} - \frac{(z - z_-)^2}{2\sigma_z^2} \right) \dots \quad (S12)$$

The normalization factors (A_+ and A_-) are used to impose the integrated charge on the centroid to be equal to the corresponding density change integrated in the whole space:

$$A_+ = \frac{\int \rho_+(r) dr}{\int e(-\frac{(x - x_+)^2}{2\sigma_{+x}^2} - \frac{(y - y_+)^2}{2\sigma_{+y}^2} - \frac{(z - z_+)^2}{2\sigma_{+z}^2}) dr} \dots \quad (\text{S13})$$

$$A_{\perp} = \frac{\int \rho_{\perp}(r) dr}{\int e(-\frac{(x - x_{\perp})^2}{2\sigma_{\perp x}^2} - \frac{(y - y_{\perp})^2}{2\sigma_{\perp y}^2} - \frac{(z - z_{\perp})^2}{2\sigma_{\perp z}^2}) dr} \quad \dots \dots \dots \text{(S14)}$$

H index is defined as half of the sum of the centroids axis along the D–A direction, if the D–A direction is along the X axis, H is defined by the relation:

$$H = \frac{\sigma_{+x} + \sigma_{-x}}{2} \quad \dots \dots \dots \text{(S15)}$$

The centroid along X axis is expected. The t intex represents the difference between D_{CT} and H:

$$t = D_{CT} - H \quad \dots \dots \dots \text{(S16)}$$

SI-III: Figures

Figure S1: Computed hole and particle distribution of MPPIS-Cz and MPPIS-TPA for S_1 - S_5 ; green and blue areas represents increased and decreased electron density, respectively.

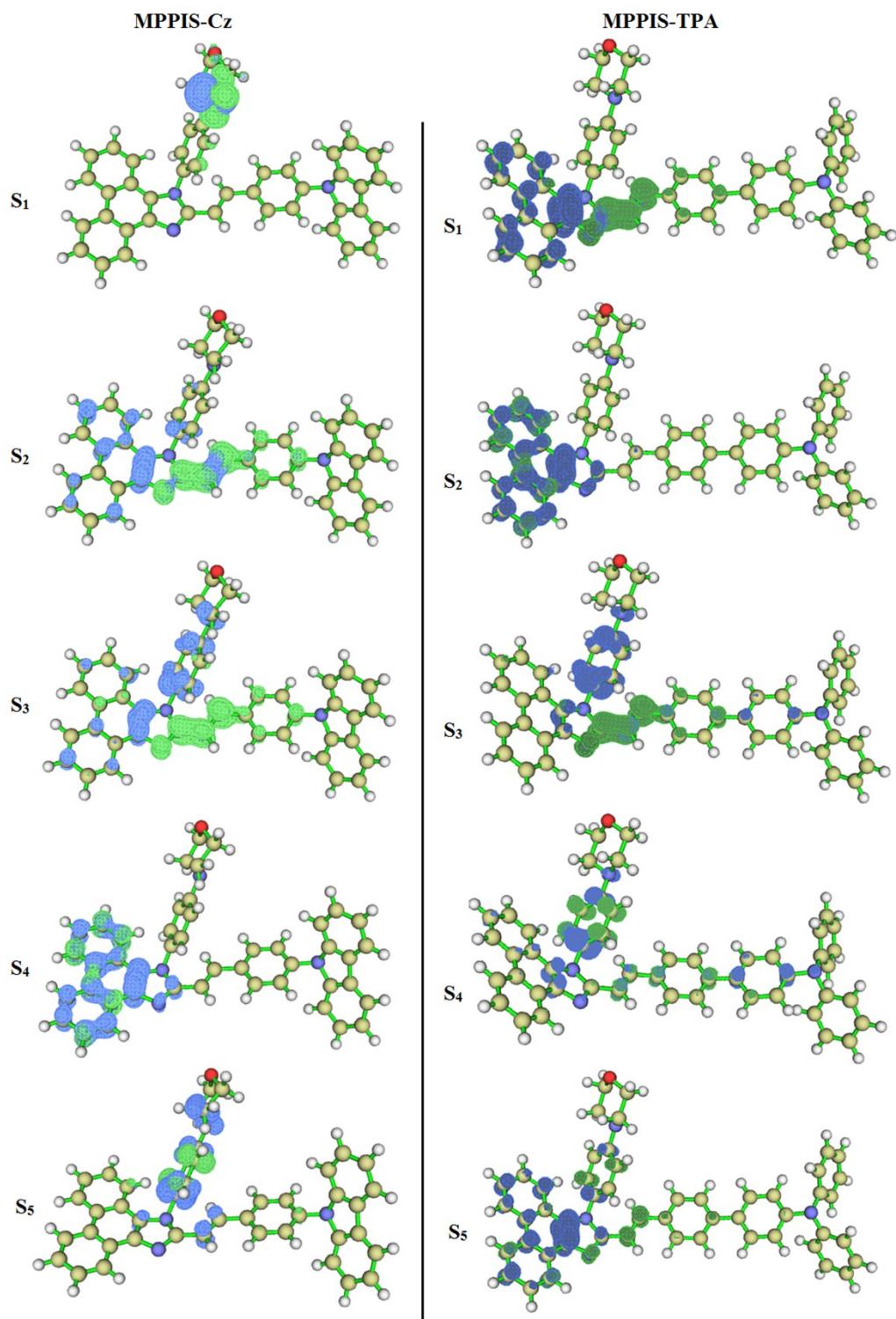


Figure S2: Contour plots of transition density matrices (TDM) of MPPIS–Cz for S_1 – S_5 states.

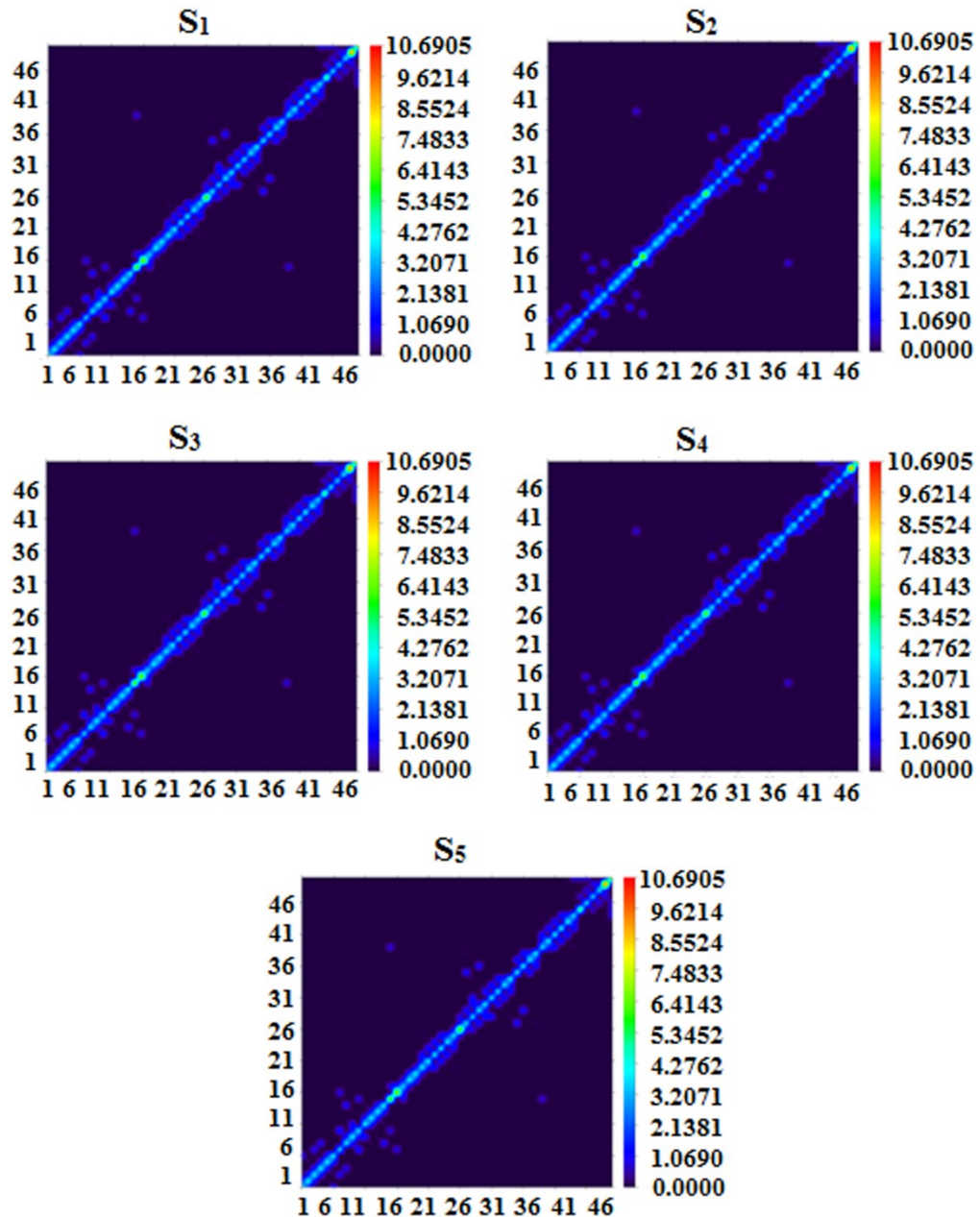


Figure S3: Contour plots of transition density matrices (TDM) of MPPIS–TPA for S_1 – S_5 states.

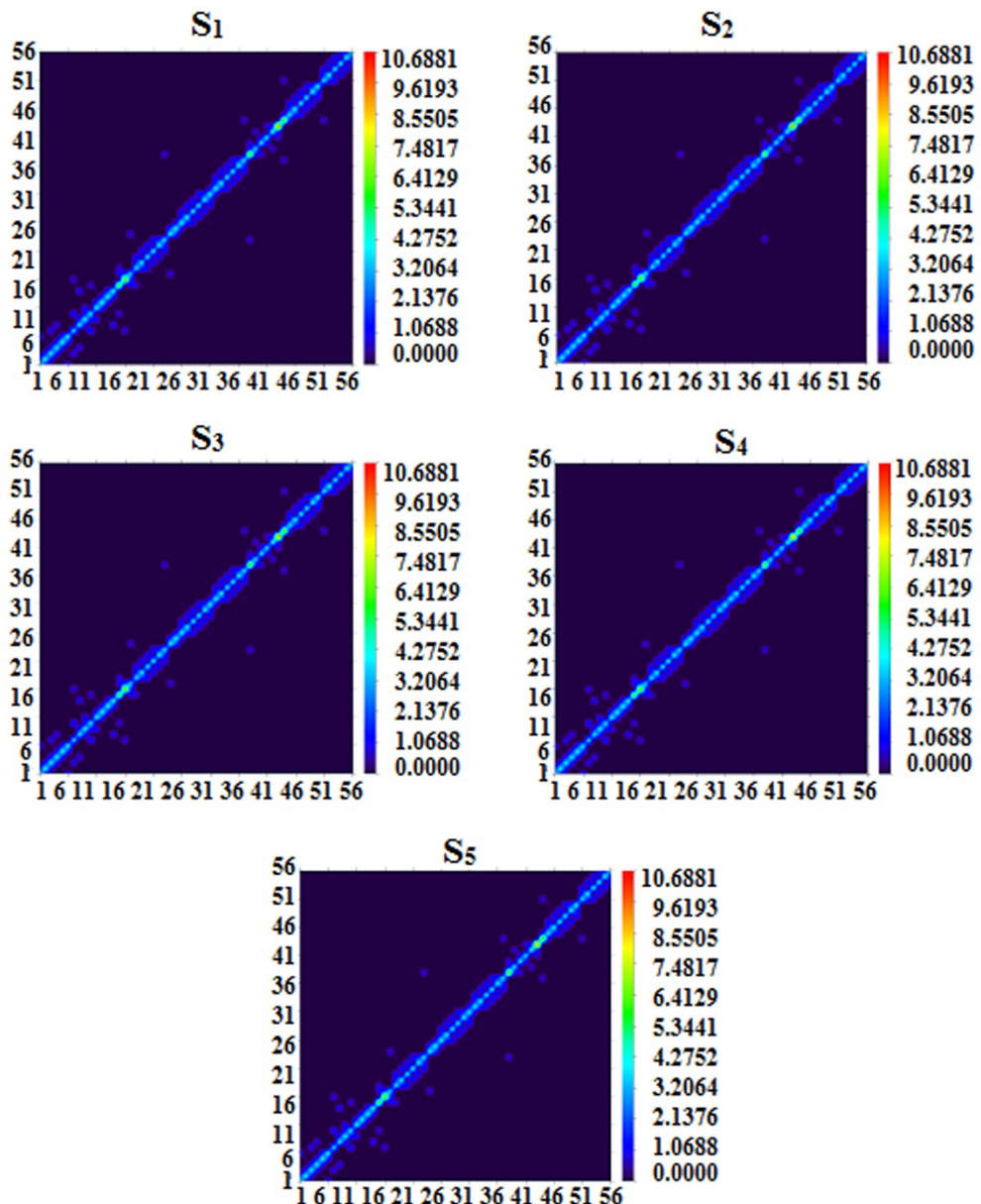


Figure S4: Normalized absorption (a and b) and emission spectra (c and d) of MPPIS–Cz and MPPIS–TPA.

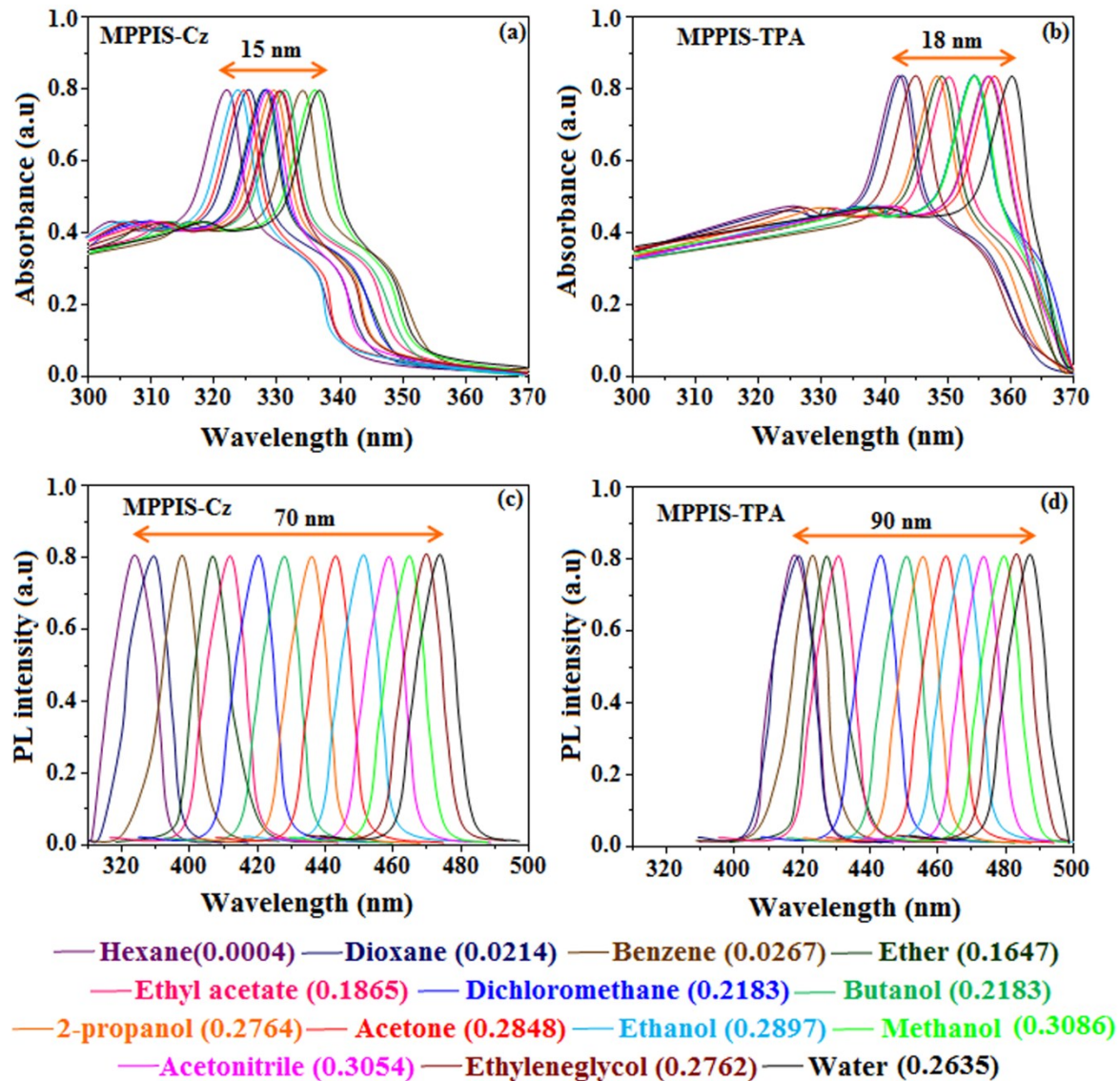


Figure S5: Radiative transition rates (k_r) and non-radiative transition rates (k_{nr}) of MPPIS-TPA and MPPIS-Cz.

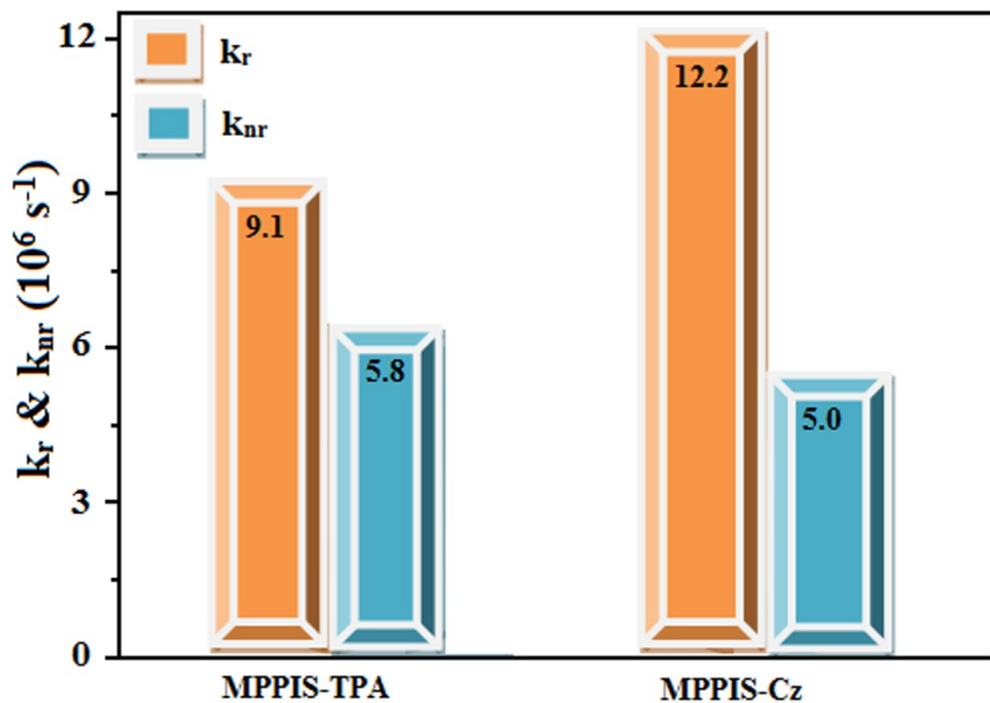
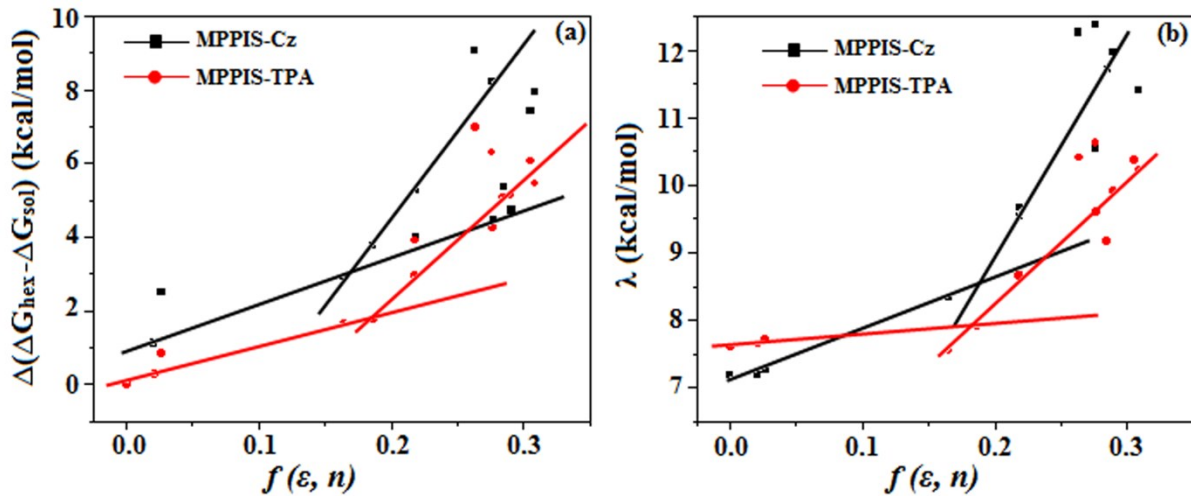
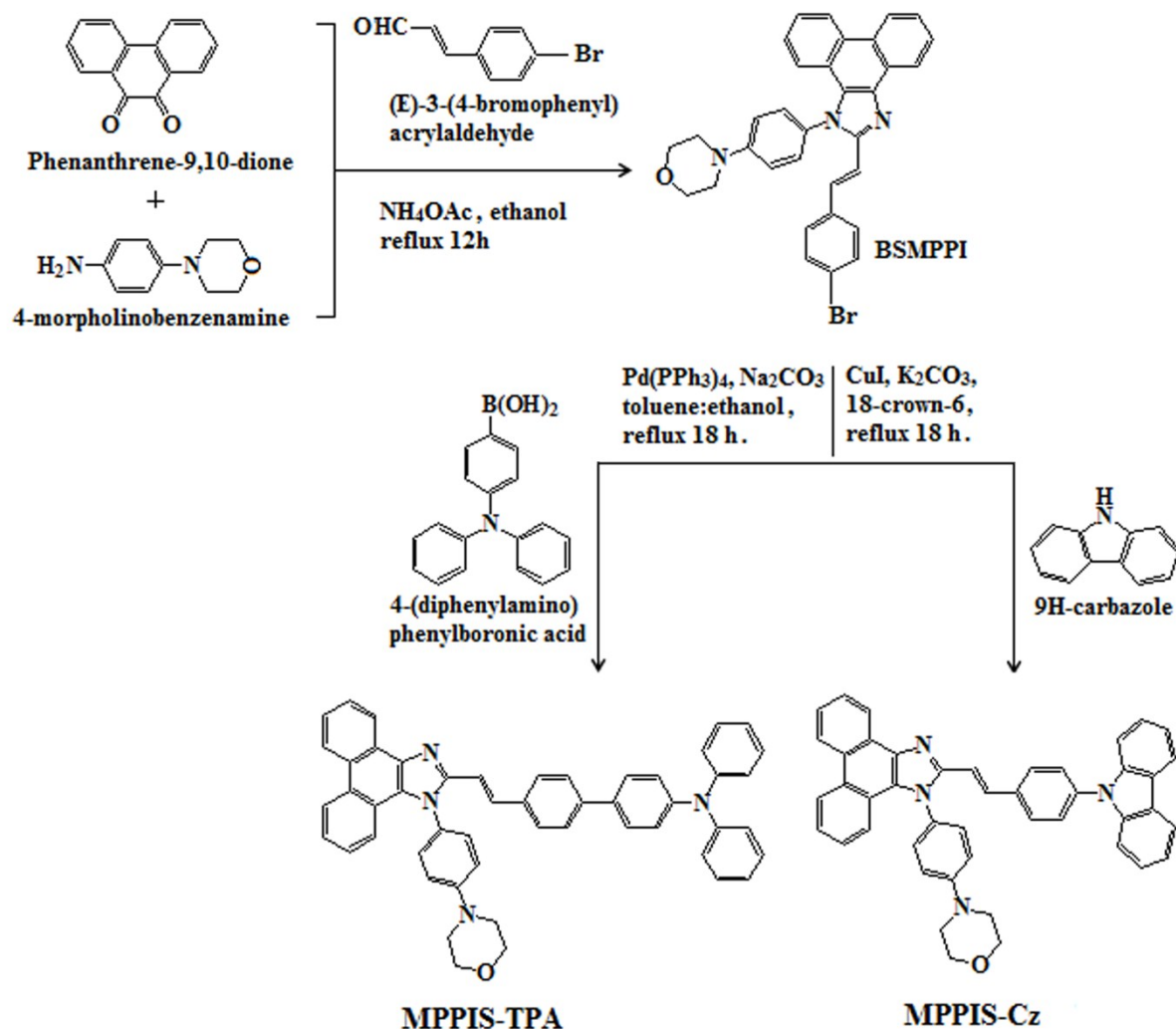


Figure S6: (a) Plot of $\Delta (\Delta G_{\text{hex}} - \Delta G_{\text{sol}})$ versus solvent polarity function, $f(\varepsilon, n)$ of MPPIS-Cz and MPPIS-TPA; (b) Plot of λ_0 depend on the solvent polarity function, $f(\varepsilon, n)$ of MPPIS-Cz and MPPIS-TPA.

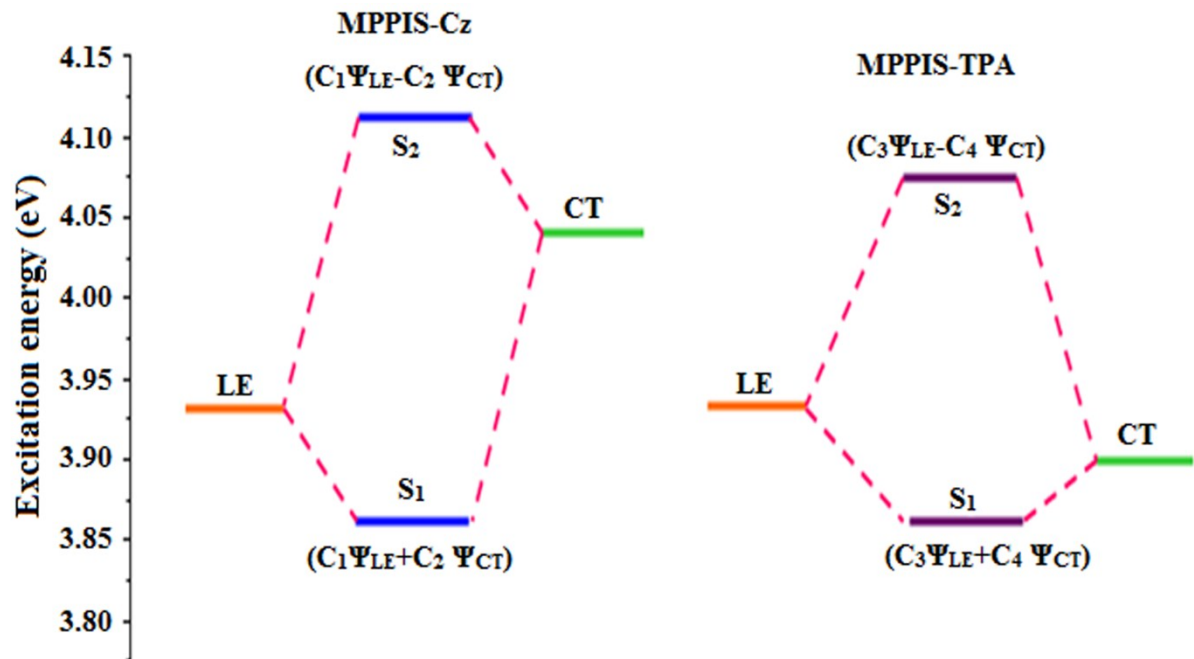


SI-IV: Schemes

Scheme S1. Synthetic route of MPPIS-Cz and MPPIS-TPA



Scheme S2. Schematic diagram of hybridization processes of LE and CT states of MPPIS-Cz and MPPIS-TPA



SI-V: Tables**Table S1:** Computed oscillator strength (f), dipole moment (μ , D) and singlet-triplet energy difference (ΔE_{ST} , eV) of MPPIS-Cz and MPPIS-TPA from NTOs

States	MPPIS-Cz			MPPIS-TPA		
	f	μ	ΔE_{ST}	f	μ	ΔE_{ST}
S1	0.76	3.31	0.99	0.61	3.43	0.8
S2	0.11	1.33	0.23	0.07	0.85	0.32
S3	0.04	0.84	0.08	0.19	1.07	0.23
S4	0.26	1.45	0.16	0.50	2.06	0.12
S5	0.47	2.12	0.28	0.10	0.95	0.22

Table S2: Computed excitation energy (eV), excitation coefficient and Δr intex (\AA) for first five singlet–triplet states of MPPIS–Cz and MPPIS–TPA.

Blue emissive materials	States	Singlet			Triplet		
		Excitation energy	Excitation coefficient	Δr intex	Excitation energy	Excitation coefficient	Δr intex
MPPIS-Cz	1	3.8609	0.4482	1.6415	2.8631	0.2699	1.5092
	2	4.1095	0.3955	1.5550	3.8712	0.2898	1.4717
	3	4.1492	0.4006	1.0718	4.4048	0.2567	1.3533
	4	4.2813	0.4092	1.3105	4.4647	0.3750	2.0859
	5	4.4558	0.3492	2.0108	4.5166	0.2435	1.4613
MPPIS-TPA	1	3.6357	0.4106	4.4238	2.8321	0.3208	4.3506
	2	3.9425	0.4147	4.2759	3.6421	0.2495	3.9578
	3	4.1166	0.3909	3.5190	3.8823	0.2607	3.6791
	4	4.2305	0.3638	3.1476	4.0964	0.1474	4.3222
	5	4.3752	0.3799	4.4551	4.1531	0.2465	3.5310

Table S3: Computed integral of hole (H) and integral of electron (E) overlap (S_{H-E}), distance between centroids of H and E (D_{H-E} , Å), integral of transition density and dipole moment (μ , a.u) for S_1-S_5 states of MPPIS–Cz and MPPIS-TPA.

Blue emissive materials	States	H	E	Transition density	S_{H-E}	Centroid of H (Å)			Centroid of E (Å)			D_{H-E}	μ
						x	y	z	x	y	z		
MPPIS-Cz	S1	0.77	0.45	0.004	0.15	-0.96	4.34	1.28	-0.59	3.91	1.28	0.56	14.78
	S2	0.81	0.65	0.009	0.33	-3.08	-1.10	-0.18	-1.15	-1.41	-0.36	1.96	13.84
	S3	0.82	0.65	0.006	0.22	-3.12	-0.04	-0.12	-1.34	-1.25	-0.34	2.15	15.76
	S4	0.86	0.63	-0.001	0.53	-5.29	-1.54	0.15	-5.86	-1.45	0.13	0.56	12.96
	S5	0.70	0.5102	0.005	0.27	-1.74	1.00	-0.12	-1.52	0.79	-0.44	0.44	13.86
MPPIS-TPA	S1	0.84	0.66	0.014	0.30	5.55	-1.85	-0.05	3.25	-1.51	-0.70	2.47	23.29
	S2	0.87	0.63	0.003	0.55	6.30	-1.92	0.14	6.79	-1.81	0.23	0.51	21.20
	S3	0.81	0.63	0.006	0.28	2.29	0.11	-0.53	2.07	-1.28	-0.73	1.42	18.20
	S4	0.76	0.55	0.008	0.38	2.13	-0.37	-0.35	2.06	-0.34	-0.46	0.13	17.38
	S5	0.79	0.57	0.005	0.40	4.99	-1.39	-0.05	3.94	-1.33	-0.21	1.06	20.32

Table S4: Computed RMSD of electron and hole, H index and t index for S₁–S₅ of MPPIS–Cz and MPPIS–TPA.

Blue emissive materials	States	RMSD of electron				RMSD of hole				H index		t index		
		x	y	z	total	x	y	z	total	x	y	z	total	
MPPIS-Cz	S1	1.034	1.665	1.007	2.203	0.918	1.069	0.842	1.641	1.917	-0.613	-0.932	-0.925	1.449
	S2	2.983	1.320	0.835	3.367	3.450	1.777	0.937	3.992	3.678	-1.286	-1.236	-0.700	1.917
	S3	2.938	1.537	0.877	3.430	2.536	2.406	0.998	3.636	3.501	-0.961	-0.783	-0.710	1.429
	S4	1.849	2.026	1.095	2.954	2.228	2.015	1.069	3.189	3.068	-1.480	-1.940	-1.066	2.663
	S5	2.734	1.709	1.106	3.409	2.519	2.341	1.056	3.597	3.448	-2.404	-1.818	-0.761	3.108
MPPIS-TPA	S1	3.164	1.425	0.940	3.595	3.564	1.691	1.055	4.083	3.839	-1.065	-1.225	-0.343	1.659
	S2	2.827	2.101	1.069	3.681	3.177	1.939	1.069	3.873	3.773	-2.509	-1.909	-0.979	3.301
	S3	3.811	1.439	0.903	4.172	4.360	2.027	0.939	4.899	4.532	-3.861	-0.341	-0.721	3.943
	S4	4.598	1.980	1.075	5.120	5.127	2.070	1.002	5.619	5.369	-4.790	-1.996	-0.929	5.272
	S5	4.317	2.162	1.163	4.967	4.299	2.098	1.068	4.901	4.934	-3.258	-2.069	-0.955	3.976

Table S5: Transferred charges (q_{CT}), barycentres of electron density loss (R_+) / gain (R_-), distance between two barycenters (D_{CT}), dipole moment of CT (μ_{CT}), RMSD of +ve / -ve parts, CT indices (H & t) and overlap integral of C+ / C- of MPPIS-Cz and MPPIS-TPA

Blue emissive materials	$q_{CT} e^{-1} $	$R_+ (\text{\AA})$			$R_- (\text{\AA})$			$D_{CT} (\text{\AA})$	$\mu_{CT} (\text{D})$	$(+ve) \text{ RMSD}$	$(-ve) \text{ RMSD}$	$H / t (\text{\AA})$	$(C+/ C-)$
		x	y	z	x	y	z						
MPPIS-Cz	157.9-113.7	-0.23	0.31	0.041	-0.66	0.18	0.13	0.469	348.3	11.9	11.7	6.3/5.8	0.9939
MPPIS-TPA	156.5-112.5	-0.06	-0.09	0.001	-0.44	0.35	-0.09	0.607	179.9	14.1	13.2	7.2/6.6	0.9795

Table S6: Photophysical properties of MPPIS–Cz in different solvents.

Solvents	ϵ	n	f(ϵ, n)	ET(30)	λ_{abs} (nm)	ν_{abs} (cm $^{-1}$)	λ_{emi} (nm)	ν_{emi} (cm $^{-1}$)	ν_{ss} (cm $^{-1}$)	ΔG (kcal/mol)	$\Delta (\Delta G_{\text{hex}} - \Delta G_{\text{sol}})$ (kcal/mol)	λ (kcal/mol)
Hexane	1.88	1.3700	0.000411	32.4	322	31055.90	384	26041.67	5014.234	81.61	0.00	7.17
Dioxane	2.22	1.4226	0.021437	36.0	326	30674.85	390	25641.03	5033.821	80.49	1.12	7.19
Benzene	2.28	1.4260	0.026639	34.3	331	30211.48	398	25125.63	5085.852	79.09	2.52	7.27
Ether	4.27	1.3526	0.164721	34.5	328	30487.80	407	24570.02	5917.780	78.69	2.92	8.46
Ethyl acetate	6.09	1.4131	0.186569	38.1	331	30211.48	412	24271.84	5939.636	77.87	3.74	8.49
Dichloromethane	9.08	1.4242	0.218349	40.7	328	30487.80	420	23809.52	6678.281	77.60	4.01	9.54
Butanol	17.40	1.3990	0.218349	49.7	332	30120.48	428	23364.49	6755.996	76.44	5.17	9.66
2-propanol	20.18	1.3780	0.276378	48.4	330	30303.03	436	22935.78	7367.250	76.09	5.52	10.53
Acetone	21.01	1.3588	0.284780	42.2	325	30769.23	443	22573.36	8195.867	76.24	5.37	11.71
Ethanol	25.30	1.3611	0.289727	51.9	324	30864.20	451	22172.95	8691.249	75.80	5.81	12.42
Methanol	33.00	1.3288	0.308634	55.4	336	29761.90	459	21786.49	7975.412	73.68	7.93	11.40
Acetonitrile	37.50	1.3442	0.305378	45.6	329	30395.14	465	21505.38	8889.760	74.18	7.43	12.71
Ethyleneglycol	41.40	1.4318	0.276212	55.9	334	29940.12	470	21276.60	8663.524	73.20	8.41	12.38
Water	80.34	1.3330	0.263594	63.1	337	29673.59	474	21097.05	8576.544	72.56	9.05	12.26

Table S7: Photophysical properties of MPPIS–TPA in different solvents.

Solvents	ϵ	n	f(ϵ, n)	ET(30)	λ_{abs} (nm)	ν_{abs} (cm $^{-1}$)	λ_{emi} (nm)	ν_{emi} (cm $^{-1}$)	ν_{ss} (cm $^{-1}$)	ΔG (kcal/mol)	$\Delta (\Delta G_{\text{hex}} - \Delta G_{\text{sol}})$ (kcal/mol)	λ (kcal/mol)
Hexane	1.88	1.3700	0.000411	32.4	342	29239.77	418	23923.44	5316.321	75.98	0.00	7.60
Dioxane	2.22	1.4226	0.021437	36	343	29154.52	420	23809.52	5344.995	75.70	0.28	7.64
Benzene	2.28	1.4260	0.026639	34.3	345	28985.51	424	23584.91	5400.602	75.14	0.84	7.72
Ether	4.27	1.3526	0.164721	34.5	349	28653.30	428	23364.49	5288.809	74.35	1.63	7.56
Ethyl acetate	6.09	1.4131	0.186569	38.1	348	28735.63	431	23201.86	5533.776	74.23	1.75	7.91
Dichloromethane	9.08	1.4242	0.218349	40.7	350	28571.43	444	22522.52	6048.906	73.03	2.95	8.65
Butanol	17.40	1.3990	0.218349	49.7	354	28248.59	451	22172.95	6075.639	72.07	3.91	8.68
2-propanol	20.18	1.3780	0.276378	48.4	354	28248.59	456	21929.82	6318.763	71.72	4.26	9.03
Acetone	21.01	1.3588	0.284780	42.2	357	28011.20	463	21598.27	6412.932	70.90	5.08	9.17
Ethanol	25.30	1.3611	0.289727	51.9	354	28248.59	469	21321.96	6926.626	70.85	5.13	9.90
Methanol	33.00	1.3288	0.308634	55.4	354	28248.59	474	21097.05	7151.541	70.53	5.45	10.22
Acetonitrile	37.50	1.3442	0.305378	45.6	356	28089.89	480	20833.33	7256.554	69.92	6.06	10.37
Ethyleneglycol	41.40	1.4318	0.276212	55.9	356	28089.89	484	20661.16	7428.731	69.68	6.30	10.62
Water	80.34	1.3330	0.263594	63.1	360	27777.78	488	20491.80	7285.974	68.99	6.99	10.41

REFERENCES

- [1] J. M. Foster and S. F. Boys, *Rev. Mod. Phys.*, 1960, **32**, 300-302.
- [2] S. F. Boys, *Rev. Mod. Phys.*, 1960, **32**, 296-299.
- [3] H. Fang, J. Bian, L. Li and W. J. Yang, *Chem. Phys.*, 2004, **120**, 9458-9466.
- [4] Q. A. Smith, K. Ruedenberg, M. K. Gordon and L. V. Slipchenko, *J. Chem. Phys.*, 2012, **136**, 244107-12.